Data
Models
Inventories

PARIS

Process Attribution of Regional Emissions

GA 101081430, RIA

Inverse estimates of nitrous oxide emissions

Milestone 20			
Delivery due date Annex I	April 2024		
Actual date of submission	October 2024		
Lead beneficiary: Empa	Work package: 5	Nature: data	Dissemination level: Public
Responsible scientist	S. Henne		
Contributors	S. Henne, Empa, A. Manning, MO A. Ganesan, UNIVBRIS		
Internal reviewers	-		
Version: 1			

Horizon Europe Cluster 5: Climate, energy and mobility

"This project has received funding from the European Union's Horizon Europe Research and Innovation programme under HORIZON-CL5-2022-D1-02 Grant Agreement No 101081430 - PARIS".

Table of content

1. Changes with respect to the DoA (Description of the Action)

N/A

2. Dissemination and uptake

This output and/or the methods developed leading to this output will be used in compiling the annexes to the upcoming National Inventory Documents (NID). This output is used in WP2 for the reconciliation of top-down and bottom-up national level estimates, and in discussion with stakeholders and national inventory report compilers. Furthermore, it will be used within WP5 to compare to N_2O emission estimates of biogeochemical models (Task 5.6).

3. Short Summary of results

Close collaboration between the three modelling groups in the project, University of Bristol, Met Office and EMPA, has resulted in a standardized data format for the output of the inverse models. An intercomparison software tool has been developed across the groups, which allows detailed investigation of the different modelling systems to be conducted efficiently and in-depth.

The development of both this tool and the three models to output the required information, was carried out by modelling N_2O, which is measured at around 30 existing European sites. This allowed us to gain an understanding of modelling differences and to make changes to the models, where necessary. This tool, and the inverse models, have been used to explore inverse modelling of N_2O using monthly a posteriori results covering the period 2018–2023. Inversions have been completed using the three inversion systems: InTEM, ELRIS, and RHIME using atmospheric transport simulations provided by the NAME model. Furthermore, ELRIS was also run with output from the atmospheric transport model FLEXPART. An in-depth intercomparison of the results generated by the different models has been conducted. The data became publicly available by linkage with the NID annexes.

4. Evidence of accomplishment

4.1 Introduction | Background of the milestone

Inverse estimates of N_2O are made using atmospheric measurements of mole fractions. Use of atmospheric transport models is necessary to translate these atmospheric measurements into estimates of emissions from the surface. Multiple methods and analyses can be used to couple models with atmospheric data, which can vary significantly, for example through the data filtering methodologies, resolution of the transport model output, transport model setup, and execution of the statistical inversion technique.

Team members have each published their own independent methods and results on the use of their inversion systems in estimating greenhouse gas emissions (e.g., Manning et al., 2021, Redington et al., 2023, Katharopoulos et al., 2023). PARIS aims to understand the differences between setups, the effects of those differences, and harmonising, where possible, the inputs and outputs to allow for robust comparability.

Throughout the project, N_2O emissions estimates will be derived for Europe across a matrix of transport models and inversion setups through this project, using new data also collected in the project.

- University of Bristol: RHIME-NAME, RHIME-FLEXPART
- Met Office: InTEM-NAME InTEM-FLEXPART
- EMPA: ELRIS-NAME and ELRIS-FLEXPART

4.2 Scope of the milestone

This milestone will provide inverse N_2O estimates to be used in compiling the annexes to the upcoming NID. This document reports on the progress of inversion estimates of N_2O. These estimates will be made on a recurring basis across the course of the project. This milestone report shows the progress in delivery of the systems to make these estimates together with some of the first results. The results and methodologies will feed into the NID annex work that is due later in the year. Current results are thus shown in comparison to the last available NIR (2023). In this report, we show results from measurements of N_2O using the historic and ongoing measurements across Europe, which were compiled as part of D5.1, and from the following configurations: Met Office (InTEM-NAME), the University of Bristol (RHIME-NAME), and EMPA (ELRIS-NAME, ELRIS-FLEXPART).

4.3 Content of the milestone

Significant work has been undertaken to prepare for the first national inventory comparison in autumn 2024. Intense exchange between three modelling groups (University of Bristol, Met Office, and EMPA) has resulted in standardized data formats for inverse modelling enabling the rapid interchange of atmospheric transport model (NAME, FLEXPART) and the three inverse modelling systems (RHIME, InTEM, ELRIS). Comprehensive inter-comparison software has been co-developed across the groups. This new tool enables detailed investigation of the different modelling systems to be conducted efficiently and in depth. For N_2O, monthly inverse modelling results covering the period 2007–2023 have been completed. However, different models were only able to cover shorter periods, with results from all models being available for 2018-2023, which aligns with the period of largest observational data availability. Observations from 26 surface sites across Europe were assimilated by the inversion models. All inversion models were run with NAME footprints. In addition, ELRIS inversions were repeated using FLEXPART footprints.

Fig. 1 shows the yearly (averaged) posterior flux estimates for two of the PARIS focus countries (Germany, UK), the Benelux area and for North-West Europe (Ireland, UK, France, Belgium, Luxembourg, Netherlands, Germany) as a whole. Results from individual inversion systems are presented separately, whereas UNFCCC-reported emissions are given in comparison. Across North-Western Europe a slow decrease of N_2O emissions is reported. The inversion results in general support this trend but are considerable larger than the reported results. Differences between and uncertainties of individual inversion results decreased with time, most likely due to more observations becoming available after 2018. The inversion models agree best for German N_2O emissions after 2018, showing largely overlapping posterior uncertainties and year-to-year variability.

Fig. 2 presents the monthly posterior flux estimates for the same regions but only for the years after 2018. Pronounced seasonality in emissions and year-to-year variability can be seen across all North-West Europe. Emissions are largest from spring to summer and minimum in the winter months. This seasonal signal is generally in line with the expectation of increased emissions from agricultural soil during the growing season due to a combination of increased management (fertilisation) and increased soil temperatures, potentially modulated by soil water. That the inversions pick up year-to-year variability highlights the importance of moving from single Tier 1 approaches for estimating soil emissions to more complex approaches that consider the drivers of soil emissions (Task 5.3, Task 5.4 and Task 5.6).

The spatial distribution of N_2O emissions across North-West Europe (Fig. 3) is dominated by emission hotspots in agricultural areas with intense livestock farming (Netherlands, Belgium, eastern England, north-western Germany). These areas are present in the prior emission distribution (as taken from the EDGAR inventory) and are not spatially shifted by the inversions. However, the intensity of emissions is increased by the inversions in

most of the mentioned agricultural areas. Spatial differences in posterior emissions between the inversion system are small and not systematic.

A more thorough discussion of the inversion results will be presented to the national inventory teams of the eight PARIS focus countries as part of the draft annexes and during the individual meetings with these teams.

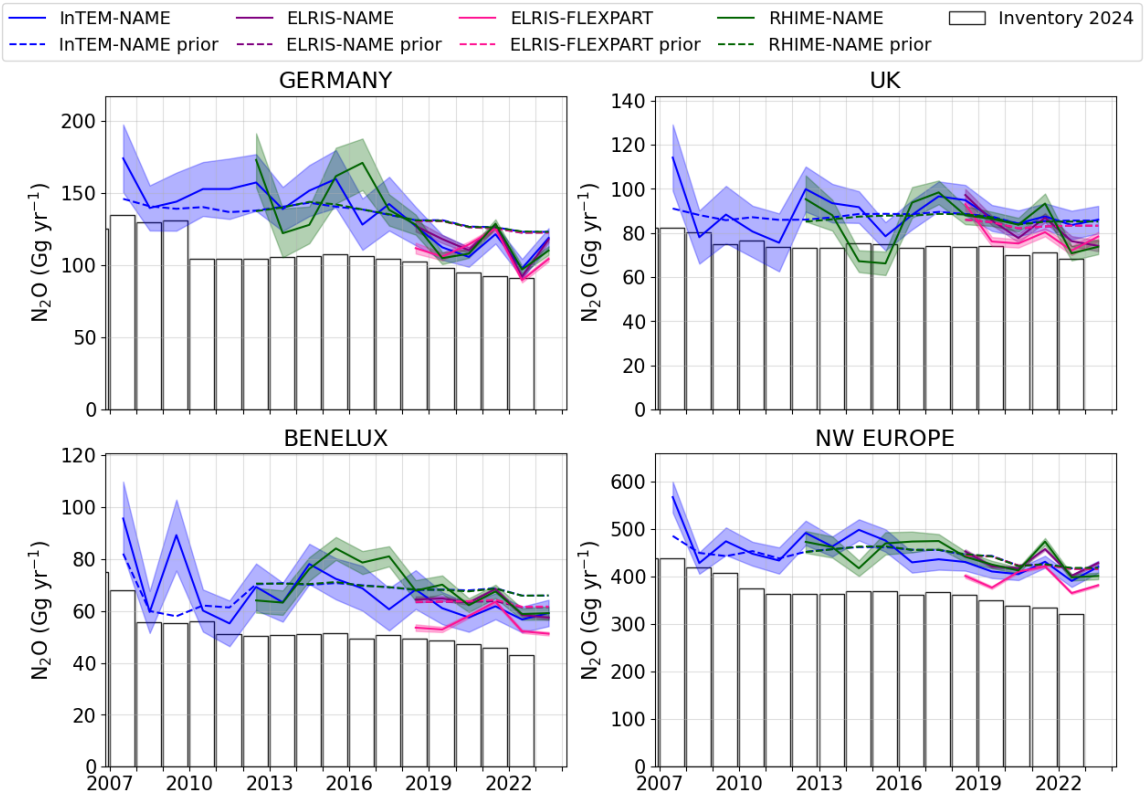

Fig. 1: Trends N_2O flux estimates (Gg y^{-1}) for different countries and regions in North-West Europe. Posterior flux estimates (solid lines) from InTEM-NAME (dark blue), ELRIS-NAME (purple), ELRIS-FLEXPART (purple), and RHIME-NAME (green), are compared to their prior flux estimates (dashed lines) and bottom-up flux estimates as reported to the UNFCCC (black bars) in 2024.

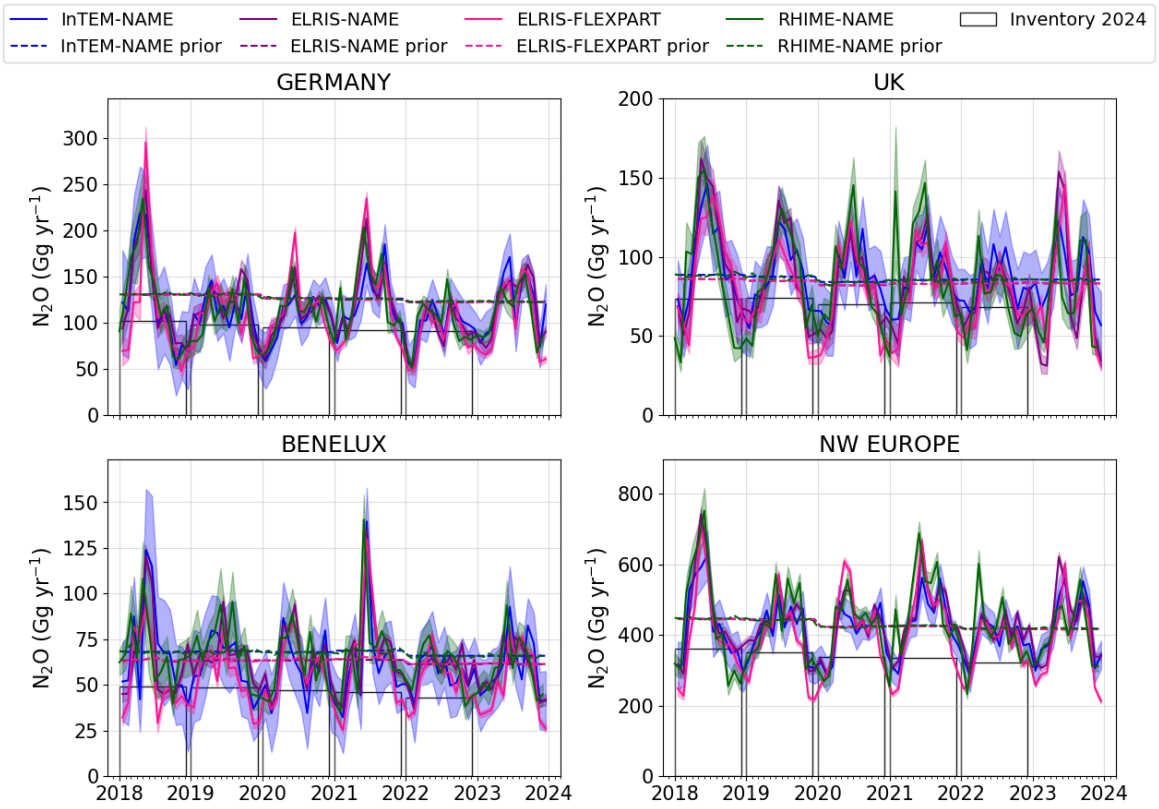

Fig. 2: Monthly N_2O flux estimates (Gg y^{-1}) for different countries and regions in North-West Europe. Posterior flux estimates (solid lines) from InTEM-NAME (dark blue), ELRIS-NAME (purple), ELRIS-FLEXPART (purple), and RHIME-NAME (green), are compared to their prior flux estimates (dashed lines) and bottom-up flux estimates as reported to the UNFCCC (black bars) in 2024.

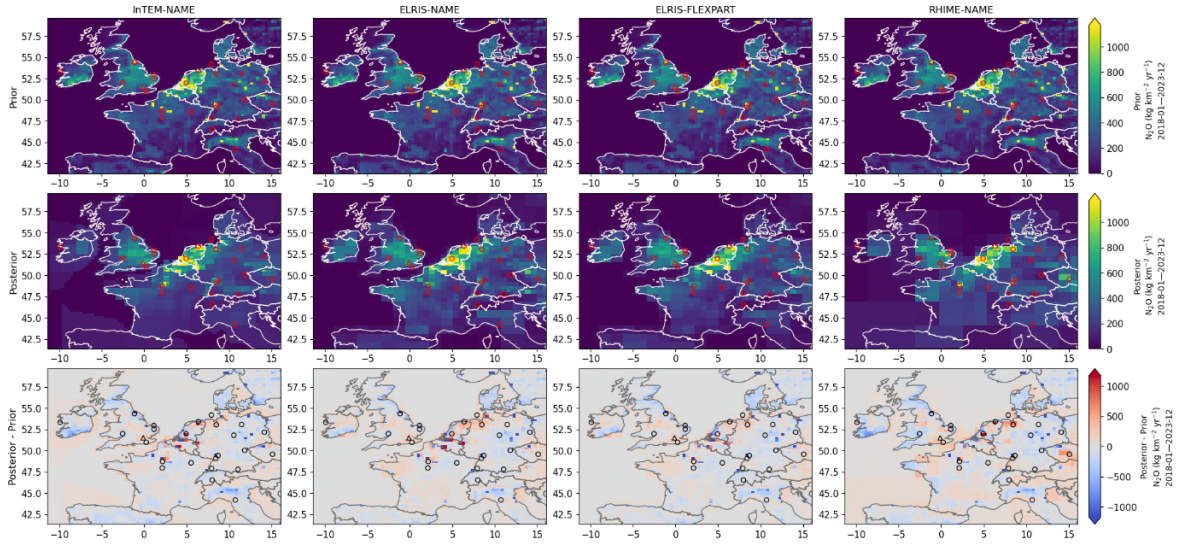

Fig. 3: Mean prior (first row) and posterior (second row) N_2O flux across North-West Europe, averaged from monthly inversions between 2018 and 2023. The third row shows the difference maps of posterior minus prior flux. Observation site locations are shown in black circles.

Fig. 4 demonstrates the performance of the inverse modelling system for the example site Hohenpeissenberg (ICOS station in southern Germany). Compared to the observations (black dots) the prior simulations (light colours) show considerable differences at different times of the year and in different ways for the four inversion runs. After the emission inversion all simulations much closer agree with the observations as documented as well through the much more narrow and more centered frequency distribution of the residuals between observations and simulations. Similar comparison statistics (bias, μ, and RMSE, σ) are obtained by all inversion systems and for the two different transport models (compare ELRIS-NAME and ELRIS-FLEXPART).

The exemplary performance demonstrated for Hohepeissenberg can also be observed for most observing sites as documented through a number of performance statistics as presented in Fig. 5 (prior) and Fig. 6 (posterior). In the prior simulations correlation coefficients between observations and simulations were generally below 0.8, mean biases were in the order of 0.5 ppb (larger for RHIME) and RMSE often larger 0.5 ppb. In contrast, correlation coefficients increased mostly above 0.8 in the posterior simulations, bias were close to zero and RMSE reduced mostly below 0.5 ppb. Some exceptions to this general rule exist for some sites. RMSE remained large for the two Dutch sites Cabauw (CBW) and Lutjeward (LUT) as well as for the Hungarian site Hegyhátsál (HUN). These sites are located in high emission regions, potentially increasing model uncertainties due to unresolved pollution events/plumes. No systematic difference in posterior performance could be distinguished between the inversion systems. Overall, the comparison statistics confirm the general applicability of the inversion systems to European N_2O emissions.

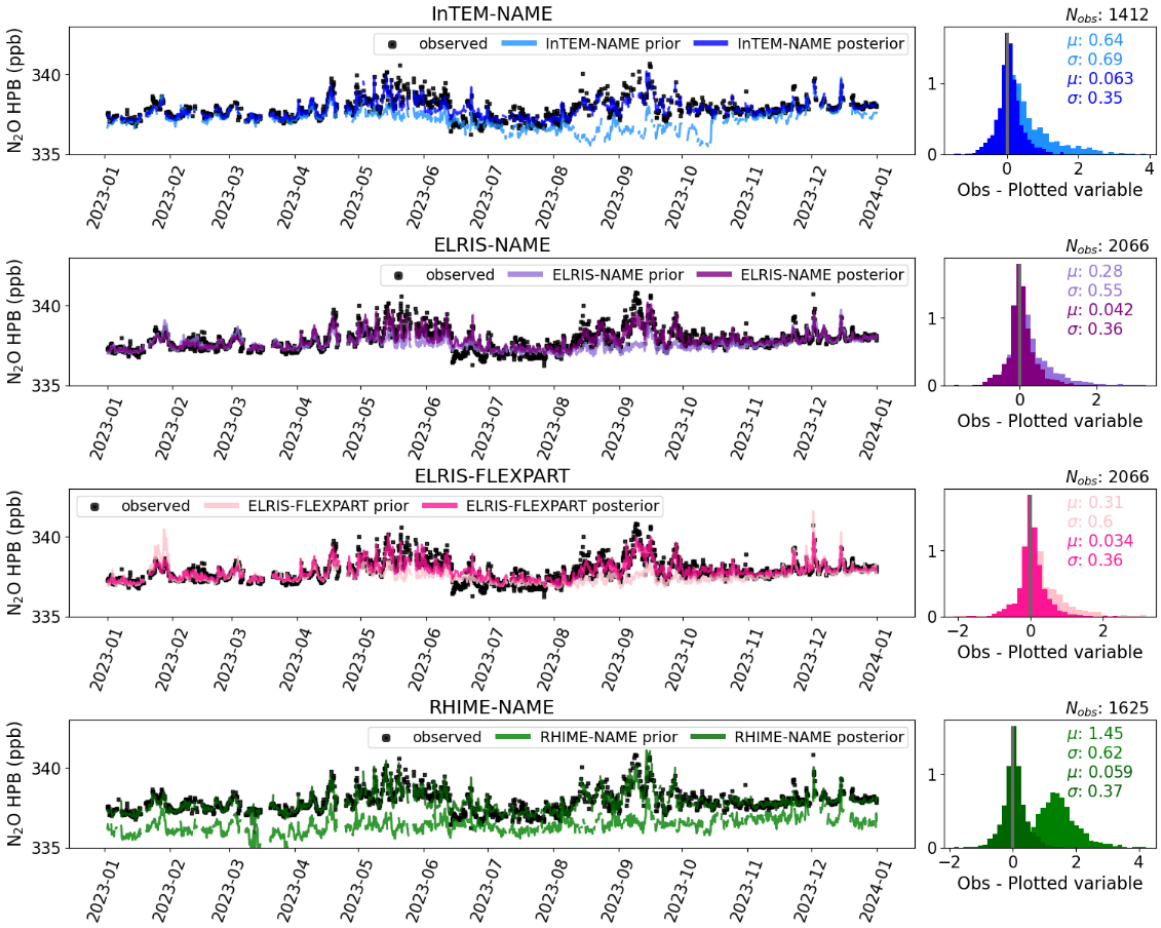

Fig. 4: One years of observed (black squares), prior (lighter colours) and posterior simulated (darker colours; dark blue: InTEM-NAME, purple: ELRIS-NAME, pink: ELRIS-FLEXPART, green: RHIME-NAME) N_2O mole fractions from the example site Hopenpeissenberg (HPB, southern Germany). Statistics representing the modelled mole fractions' fit to observations over this period are given in the histogram plots.

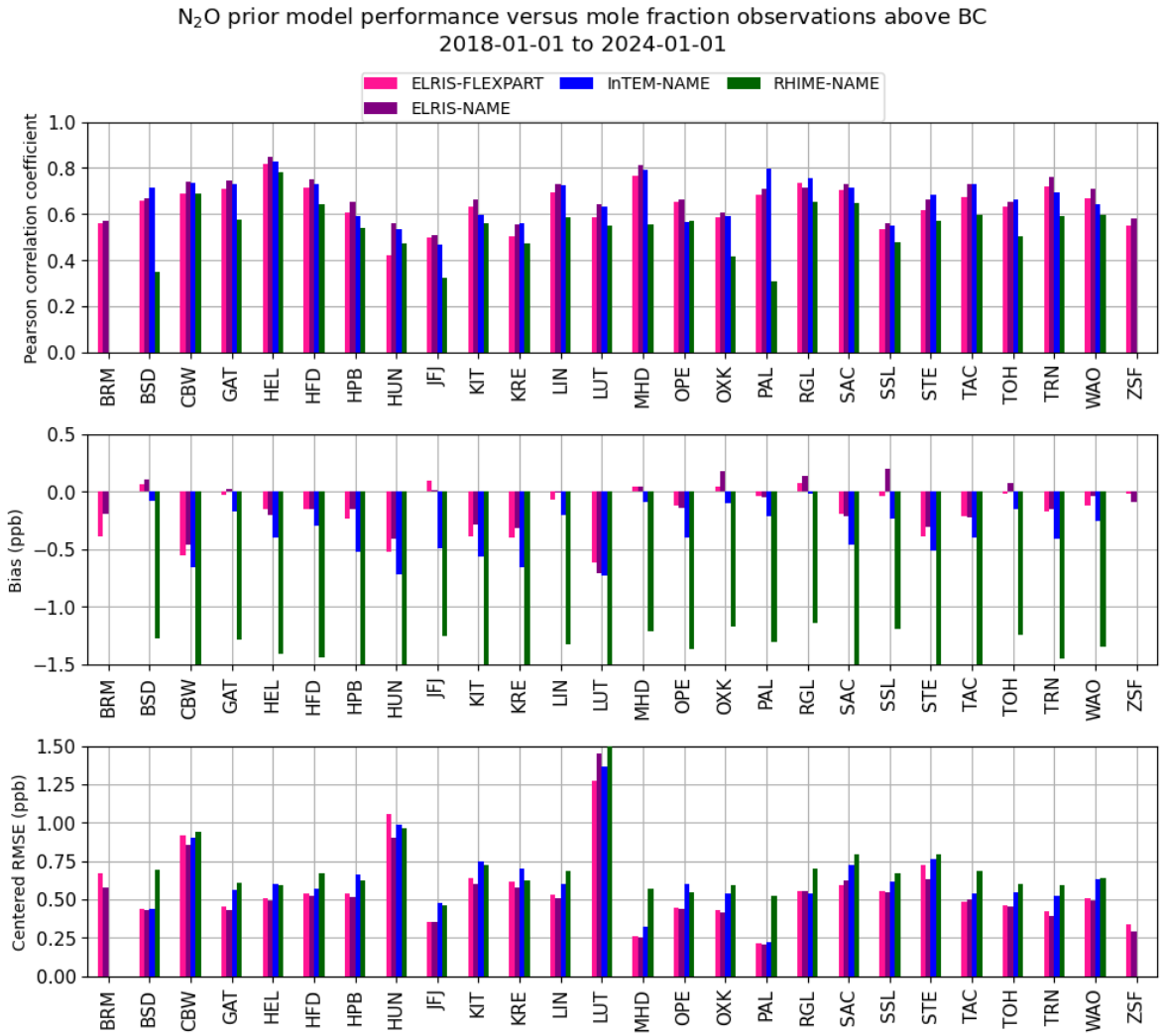

Fig. 5: Prior model performance parameters for N_2O simulations at all used observation sites and separate for all inverse models (dark blue: InTEM-NAME, purple: ELRIS-NAME, pink: ELRIS-FLEXPART, green: RHIME-NAME) for the period 2018-2023. Top: Pearson correlation coefficient; middle: mean bias; bottom: centered root mean square error (RMSE). Statistics were computed for above-background signals, removing the simulated background from both observation and simulation to avoid overestimation of correlations purely due to background trends.

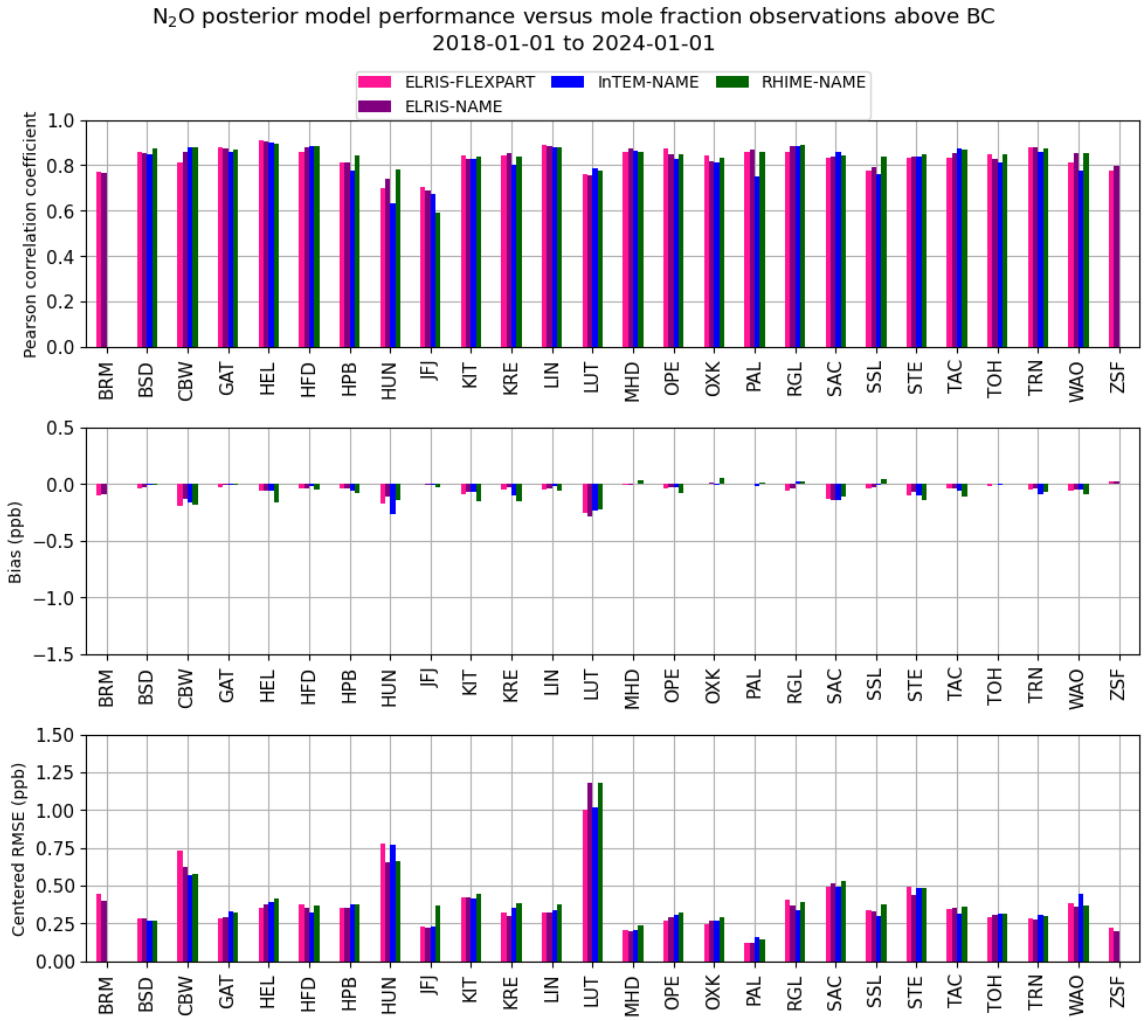

Fig. 6: Posterior model performance parameters for N2O simulations at all used observation sites and separate for all inverse models (dark blue: InTEM-NAME, purple: ELRIS-NAME, pink: ELRIS-FLEXPART, green: RHIME-NAME) for the period 2018-2023. Top: Pearson correlation coefficient; middle: mean bias; bottom: centered root mean square error (RMSE). Statistics were computed for above-background signals, removing the simulated background from both observation and simulation to avoid overestimation of correlations purely due to background trends.

4.4 Conclusion and possible impact

The initial set-up for the operational systems for inverse estimates of N_2O for Europe across the groups in this consortium is ready and results have been shown from InTEM, ELRIS, and RHIME, in preparation for later reporting under the NID annexes. For this first reporting period, a rigorous comparison between model and inversion setups have been made.

4.5 References

Manning, A. J., Redington, A. L., Say, D., O'Doherty, S., Young, D., Simmonds, P. G., Vollmer, M. K., Mühle, J., Arduini, J., Spain, G., Wisher, A., Maione, M., Schuck, T. J., Stanley, K., Reimann, S., Engel, A., Krummel, P. B., Fraser, P. J., Harth, C. M., Salameh, P. K., Weiss, R. F., Gluckman, R., Brown, P. N., Watterson, J. D., and Arnold, T.: Evidence of a recent decline in UK emissions of hydrofluorocarbons determined by the InTEM inverse model and atmospheric measurements, Atmos. Chem. Phys., 21, 12739–12755, https://doi.org/10.5194/acp-21-12739-2021, 2021

Katharopoulos, I., Rust, D., Vollmer, M. K., Brunner, D., Reimann, S., O'Doherty, S. J., Young, D., Stanley, K. M., Schuck, T., Arduini, J., Emmenegger, L., and Henne, S.: Impact of transport model resolution and a priori assumptions on inverse modeling of Swiss F-gas emissions, Atmos. Chem. Phys., 23, 14159-14186, doi: 10.5194/acp-23-14159-2023, 2023.

Redington, A. L., Manning, A. J., Henne, S., Graziosi, F., Western, L. M., Arduini, J., Ganesan, A. L., Harth, C. M., Maione, M., Mühle, J., O'Doherty, S., Pitt, J., Reimann, S., Rigby, M., Salameh, P. K., Simmonds, P. G., Spain, T. G., Stanley, K., Vollmer, M. K., Weiss, R. F., and Young, D.: Western European emission estimates of CFC-11, CFC-12 and CCl_4 derived from atmospheric measurements from 2008 to 2021, Atmos. Chem. Phys., 23, 7383–7398, https://doi.org/10.5194/acp-23-7383-2023, 2023

5. History of the document

Version	Author(s)	Date	Changes
1	Stephan Henne	4 Oct 2024	First draft